



**HAL**  
open science

## **Uplifted Holocene shorelines at Capo Milazzo (NE Sicily, Italy): Evidence of co-seismic and steady-state deformation**

G. Scicchitano, C. Spampinato, L. Ferranti, F. Antonioli, C. Monaco, M. Capano, C. Lubritto

### ► To cite this version:

G. Scicchitano, C. Spampinato, L. Ferranti, F. Antonioli, C. Monaco, et al.. Uplifted Holocene shorelines at Capo Milazzo (NE Sicily, Italy): Evidence of co-seismic and steady-state deformation. *Quaternary International*, 2011, 232 (1-2), pp.201-213. 10.1016/j.quaint.2010.06.028 . hal-01684306

**HAL Id: hal-01684306**

**<https://hal.science/hal-01684306v1>**

Submitted on 29 Apr 2019

**HAL** is a multi-disciplinary open access archive for the deposit and dissemination of scientific research documents, whether they are published or not. The documents may come from teaching and research institutions in France or abroad, or from public or private research centers.

L'archive ouverte pluridisciplinaire **HAL**, est destinée au dépôt et à la diffusion de documents scientifiques de niveau recherche, publiés ou non, émanant des établissements d'enseignement et de recherche français ou étrangers, des laboratoires publics ou privés.

# Uplifted Holocene shorelines at Capo Milazzo (NE Sicily, Italy): Evidence of co-seismic and steady-state deformation

G. Scicchitano<sup>a</sup>, C.R. Spampinato<sup>a</sup>, L. Ferranti<sup>b</sup>, F. Antonioli<sup>c</sup>, C. Monaco<sup>a,\*</sup>, M. Capano<sup>d</sup>, C. Lubritto<sup>d</sup>

<sup>a</sup> Dipartimento di Scienze Geologiche, Università di Catania, Corso Italia, 55, 95129 Catania, Italy

<sup>b</sup> Dipartimento di Scienze della Terra, Università di Napoli Federico II, Italy

<sup>c</sup> ENEA, Casaccia, Rome, Italy

<sup>d</sup> Dipartimento di Scienze Ambientali, Seconda Università di Napoli, Lab. CIRCE, Caserta, Italy

## ARTICLE INFO

### Article history:

Available online 31 July 2010

## ABSTRACT

Detailed mapping of Holocene shorelines outcropping a few meters above the present sea-level at Capo Milazzo, the main headland of NE Sicily, supplied evidence of the interplay between abrupt and steady uplift. Field analysis revealed two shorelines at distinct elevations, which were characterized through position and radiometric dating of geomorphologic and biological sea-level markers. The upper shoreline is represented by a notch, marine deposits and barnacle rims. The notch is found at average elevation of ~2.1 m above mean sea level (a.m.s.l.) and is filled by a marine deposit containing shells dated between 6.2 and 3.9 ka BP. Locally, the deposit includes pottery of Roman age (~2 ka BP). An intertidal balanid rim associated with the upper shoreline yielded ages between 3.8 and 1.6 ka BP. The lower shoreline involves a notch at ~0.8 m a.m.s.l., locally carved in the older Holocene deposit, and a likely coeval, subjacent abrasion platform at 0.5–0.6 m a.m.s.l. Remains of a balanid rim in this lower notch were dated at ~1.4 ka BP. Morphological and chronostratigraphical relations indicate that uplift of the upper shoreline occurred abruptly. Sudden displacement of 1.3–1.5 m occurred during a co-seismic event. Age and elevation relationships document that the upper shoreline was active between 6.2 and 1.6 ka, and thus co-seismic uplift must have occurred between 1.6 and ~1.4 ka, the bracketed ages of cessation and inception of the upper and lower shorelines, respectively. Using similar reasoning, a younger (~0.8–0.9 m) co-seismic uplift occurred probably shortly after 1.4 ka. These uplifts supplemented a regional, background uplift that operated steadily during the lifespan of the two shorelines. Precise compensation for the glacio-hydro-isostatic sea-level change indicated that this uplift took place at ~0.65 mm/y. Thus, cumulative uplift at the studied sites occurred at 1.2–1.5 (locally up to 2.1) mm/y, in close agreement with nearby coastal sites in Sicily and southern Calabria. Analysis suggests the occurrence of a seismogenic source in the Capo Milazzo area, possibly related to transpressive structures recently mapped offshore. The seismogenic potential of this sector of Sicily needs to be re-evaluated.

© 2010 Elsevier Ltd and INQUA. All rights reserved.

## 1. Introduction

Sea level is the general reference for detecting ongoing vertical crustal movements and assessing short- and long-term tectonic instability in coastal areas (Lajoie, 1986). Crustal movements can be detected by mapping and dating marine strandlines and separating the tectonic component from the eustatic and hydro-glacio-isostatic components of the relative sea-level change (see Lambeck et al., 2004).

Northeastern Sicily (Fig. 1) and southern Calabria are characterized by long-term uplift, as constrained by the elevation of the last

interglacial (MIS 5.5, 125 ka) terraces (Ferranti et al., 2006 and references therein). The uplift pattern of the 125 ka terrace is mirrored by the Holocene marker (Stewart et al., 1997; De Guidi et al., 2003; Antonioli et al., 2006; Ferranti et al., 2007) and has been related to a regional process, to which faulting-related deformation is added along fault-controlled coastal segments (Westaway, 1993). The uplifting region is generally associated with high-level historical seismicity (Postpischl, 1985; Boschi et al., 1995).

An anomaly in the regional seismotectonic frame is represented by Capo Milazzo, a narrow, N–S striking and about 7 km long peninsula located along the Tyrrhenian coast of northeastern Sicily (Fig. 1). Despite showing uplifted Late Quaternary shorelines (Hearty et al., 1986; Ferranti et al., 2006), it is affected by a lesser historical and instrumental seismicity.

\* Corresponding author. Tel.: +39 095 7195731; fax: +9 095 7195728.

E-mail address: cmonaco@unict.it (C. Monaco).

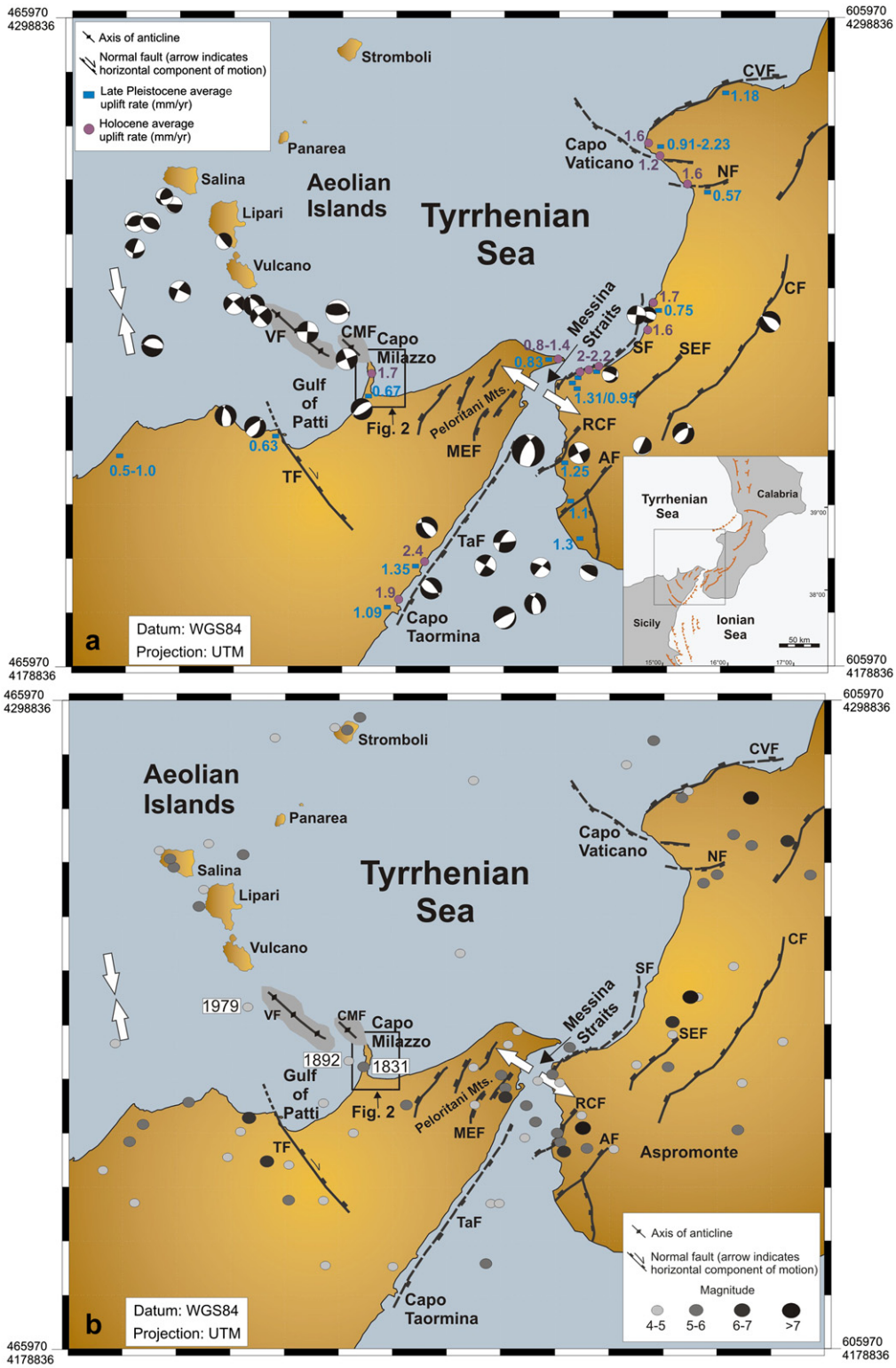


**Fig. 1.** (a) Regional tectonic map of the southern part of the Calabrian Arc. Double arrows show extension direction in Western Calabria and Eastern Sicily and contraction direction offshore northern Sicily. Active faults (rectangles on down-thrown side) after Stewart et al. (1997), Monaco and Tortorici (2000): AF, Armo fault; CF, Cittanova fault; CVF, Capo Vaticano fault; MEF, Messina fault; NF, Nicotera fault; RCF, Reggio Calabria fault; SEF, S. Eufemia fault; SF, Scilla fault; TaF, Taormina fault; TF, Tindari fault. The broad uplifted areas between Capo Milazzo and Vulcano (from Argnani et al., 2007) are indicated in grey pattern (VF, Vulcano fold; CMF, Capo Milazzo fold). Focal mechanisms of moderate to large earthquakes ( $M > 4$ ) after Harvard CMT (1976–2006) [<http://www.seismology.harvard.edu/CMTsearch.html>] and Mednet RCMT (1997–2006) [<http://mednet.ingv.it/events/QRCMT/Welcome.html>] catalogues (Pondrelli et al., 2002, 2004), Gasparini et al. (1985), and Anderson and Jackson (1987). Late Pleistocene uplift rates after Ferranti et al. (2006), Holocene uplift rates from Antonioli et al. (2009). Inset shows the tectonic setting of the Calabrian Arc. (b) Epicenters of  $M > 4$  earthquakes occurring in southern part of the Calabrian Arc between 217 BC and 2002 AD (data from CPTI04).

However, recent studies on morphological and biological sea-level markers (Rust and Kershaw, 2000; Gringeri et al., 2004) have documented that the coastal sector of the peninsula has been also uplifted during the Late Holocene, and thus deformation processes in this region may be still active today. In order to better constrain the history of recent tectonic uplifting, a detailed mapping of morphologic and biological indicators of raised Holocene shorelines over the Milazzo peninsula coastline was carried out. The main purpose of this work is to seek evidence for regional and local contributions to deformation. Resolution of mode and magnitude of partitioning of vertical crustal motion into local regional components on a very short time scale can contribute to the identification of seismogenic sources in the area.

## 2. Tectonic setting

The Capo Milazzo peninsula is located along the Tyrrhenian coast of northeastern Sicily south of the Aeolian archipelago (Fig. 1). The headland is separated by a Holocene coastal plain from the Peloritani range, the southwestern termination of the Calabrian Arc. This prominent orogenic domain connects the Apennines and the Sicilian-Maghrebian orogens that developed during the Neogene-Quaternary Africa-Europe collision (Dewey et al., 1989). The Calabrian Arc was emplaced to the south-east during north-westerly subduction and rollback of the Ionian oceanic slab (Malinverno and Ryan, 1986). Since Pliocene times, contraction structures of the inner part of the orogen were superseded by extensional faults, both longitudinal and transversal with respect to the arc, which caused the fragmentation into structural highs and marine sedimentary basins (Ghisetti and Vezzani, 1982). In eastern Sicily and Calabria, Quaternary extensional collapse at the rear of the thrust belt has accompanied a vigorous uplift recorded by flights of marine terraces (Dumas et al., 1982; Ghisetti, 1984; Valensise and Pantosti, 1992; Westaway, 1993; Miyauchi et al., 1994; Bianca et al., 1999; Catalano and De Guidi, 2003; Tortorici et al., 2003). The elevation of marine terraces and their offset across the main faults has been used to establish the relative contribution of regional and fault-related sources to uplift. According to Westaway (1993), 1.67 mm/y of post-Middle Pleistocene uplift of southern Calabria was partitioned into  $\sim 1$  mm/y due to regional processes and the residual to displacement on major faults. Shorter-term uplift rate estimates are provided by raised Holocene beaches, terraces and tidal notches (Firth et al., 1996; Stewart et al., 1997; Pirazzoli et al., 1997; Rust and Kershaw, 2000; De Guidi et al., 2003; Antonioli et al., 2003, 2006; Ferranti et al., 2007).

Uplift of the Calabrian Arc has been related to important geodynamic changes which occurred in the region since the Middle Pleistocene, signalled by the end of frontal thrust displacement and stalling of subduction of the Ionian plate beneath the orogen (Westaway, 1993; Wortel and Spakman, 2000; Goes et al., 2004). In this context, the belt between the southernmost sector of the Aeolian archipelago and northeastern Sicily, dominated by the Vulcano-Tindari fault system (also known as Tindari-Letojanni fault system; Lanzafame and Bousquet, 1997; Billi et al., 2006), currently represents a key area as it separates two different tectonic regimes (Fig. 1; Argnani et al., 2007; Mattia et al., 2008, 2009). To the east, an array of extensional faults, characterized by strong crustal seismicity and volcanism, cuts across southern Calabria and northeast Sicily (Siculo-Calabrian rift zone; Monaco and Tortorici, 2000). Active WNW-ESE extension is documented by focal mechanisms of crustal earthquakes (Pondrelli et al., 2006), structural studies (Tortorici et al., 1995; Monaco et al., 1997; Monaco and Tortorici, 2000; Jacques et al., 2001; Ferranti et al., 2007), and geodetic velocities (D'Agostino and Selvaggi, 2004; Mattia et al., 2009). To

the west of the Vulcano-Tindari fault system, the southern Tyrrhenian Sea margin is characterized by moderate crustal seismicity. Focal mechanisms mostly show strike-slip and reverse-oblique kinematics compatible with low-dip  $\sim$ NNW-SSE trending  $p$ -axes (Frepoli and Amato, 2000; Neri et al., 2005; Pondrelli et al., 2006; Giunta et al., 2009), roughly consistent with the general convergence between the European and the African plates (Hollenstein et al., 2003; Lavecchia et al., 2007; Ferranti et al., 2008).

Kinematic changes also occur along the Vulcano-Tindari fault system, which is formed by NW-SE-oriented en-echelon segments characterized by prevailing right lateral strike-slip movements in the offshore sector (Ventura, 1994; Mazzuoli et al., 1995) and by transtensional kinematic onshore (Ghisetti, 1979). Fault-plane solutions of crustal earthquakes reveal reverse focal mechanisms between Salina and Vulcano islands, dextral strike-slip mechanisms between Vulcano and Capo Milazzo and prevailing normal faulting coupled with dextral transcurrent in Gulf of Patti area (Neri et al., 2005). This kinematic framework has been recently confirmed by GPS velocity fields (Mattia et al., 2008). According to Argnani et al. (2007), the southern sector of the Aeolian archipelago between Capo Milazzo and the island of Vulcano is characterized by a NW-SE trending belt of transpressive (e.g. positive flower) structures. Along this belt, seismic profiles show the occurrence of two overstepping broad anticlines, Capo Milazzo and Vulcano folds (Fig. 1). According to the authors, transpressional deformation has occurred since the Middle Pleistocene and is superposed on a pre-existing extensional deformation. Despite these evidences, the area around Capo Milazzo and west of it shows low instrumental (Fig. 1a) and historical (Fig. 1b) seismicity, in sharp contrast with the Messina Straits area.

The summit of Capo Milazzo peninsula is characterized by a wide marine terrace extending at an elevation between 50 and 85 m. The bedrock is formed by metamorphic rocks unconformably covered by Upper Miocene reef limestones and Upper Pliocene-Lower Pleistocene marls and marly limestones (Fig. 2). Upper Pleistocene littoral mollusc-rich deposits overlying this terrace have been attributed to MIS 5.5 (Hearty et al., 1986) and indicate the Late Quaternary uplift of the whole area. Evidence of Holocene uplift was published in recent studies. In detail, Rust and Kershaw (2000) mapped two distinct notches at 0.5 and 2 m a.m.s.l. in the northernmost sector of the peninsula, assigning an age of  $\sim 5$  ka to the upper marker on the basis of regional correlations and suggesting an uplift rate close to 1 mm/y. Gringeri et al. (2004) report a radiometric age (5919–6079 cal BP) of *Patella* sp. collected at 2 m a.m.s.l. from the eastern shore of the peninsula (Punta Rugno; Fig. 2). The age was compared to the Holocene sea-level curve of Lambeck et al. (2004) and allowed the authors to determine an average uplift rate of 1.66 mm/y in the last 6 ka.

## 3. Holocene markers and radiometric ages

Detailed mapping around the coast of Capo Milazzo confirmed the existence of the uplifted shorelines described by Rust and Kershaw (2000), found evidence of other markers such as marine deposits and barnacle rims, and retrieved material for shoreline dating. Precise measurements of the heights of notches, marine deposits and barnacle rims with respect to current sea level at the time of the survey were performed with a rod (invar alloy) mechanical system. In the following, elevations will be reported with respect to the present sea level. Measurements have been corrected for tide and pressure relative to the mean sea level (MSL), using data from the tide gauges of Catania [www.wxtime32.com](http://www.wxtime32.com) and from the meteorological site [www.wunderground.com](http://www.wunderground.com).

Holocene sea-level markers occur at two distinct elevations, which are referred in the following as “upper shoreline” and “lower



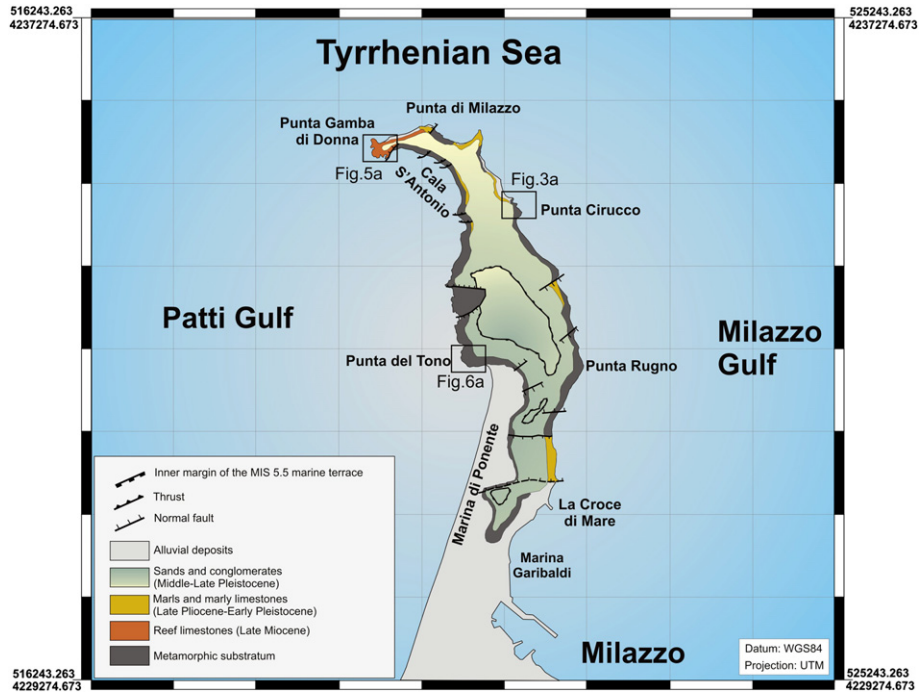


Fig. 2. Geological map of Capo Milazzo (after Lentini et al., 2000) with location of investigated Holocene sites (see Fig. 1 for location).

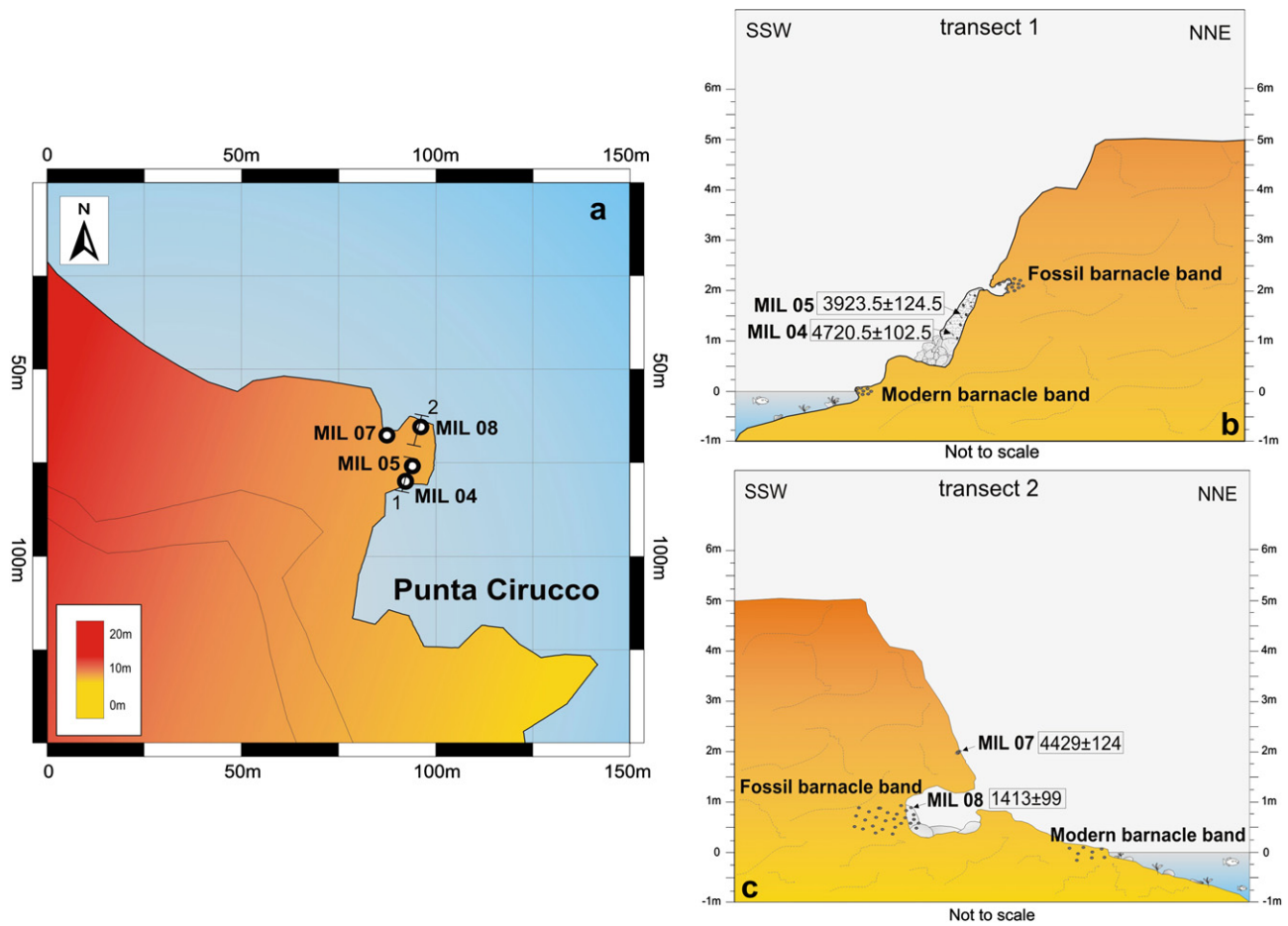
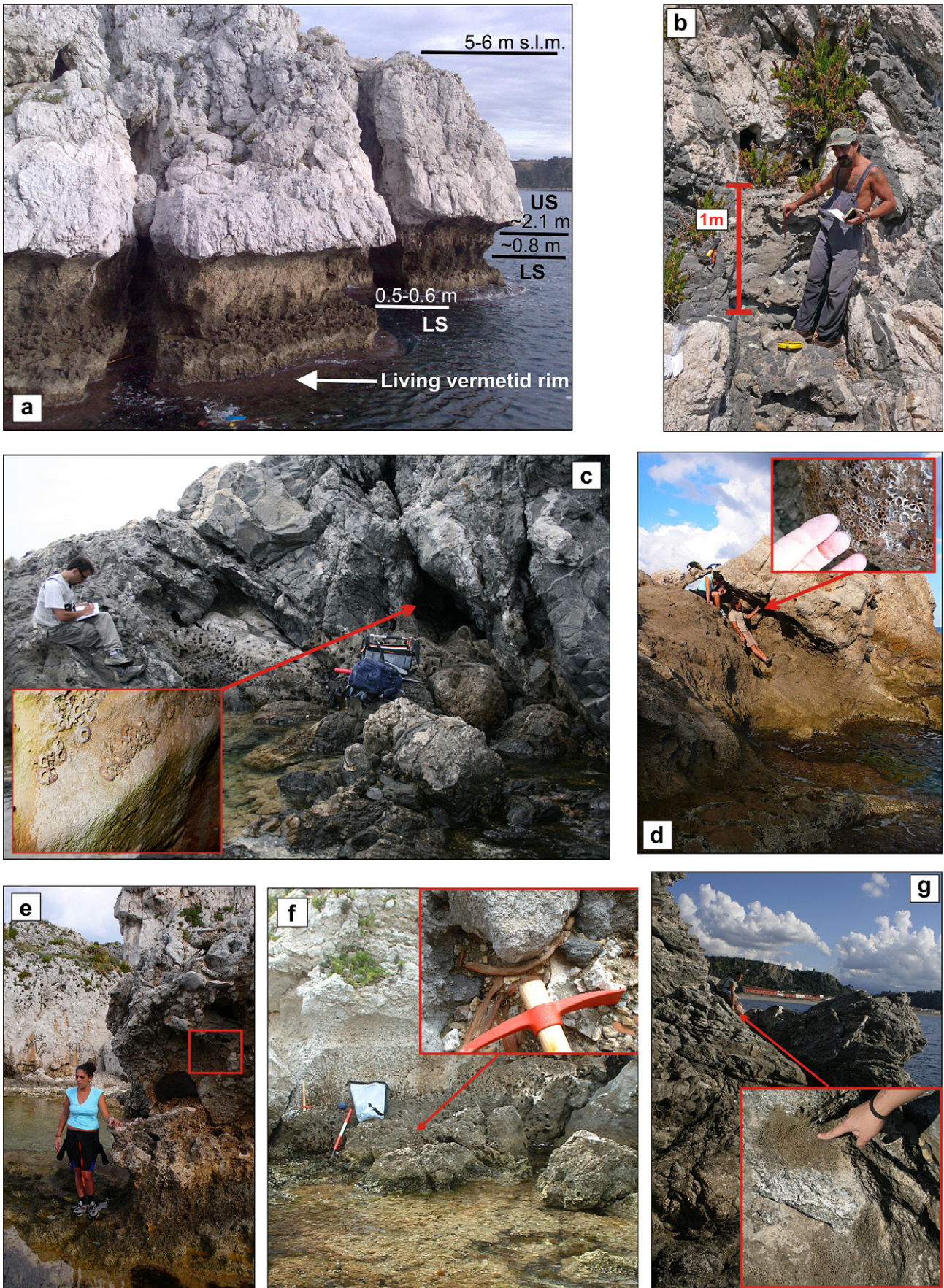


Fig. 3. (a) Sketch map of Punta Ciruccio site (see Fig. 2 for location) with location of Holocene sea-level markers (refs. Table 1). (b) Sketch profile along the southern sector of Punta Ciruccio showing the morphological and biological features of the upper shoreline, their elevation above the present mean sea level and the radiometric ages of sampled organisms. (c) Sketch profile along the northern sector of Punta Ciruccio showing the morphological and biological features of the lower shoreline, their elevation above the present mean sea level and the radiometric ages of sampled organisms.





**Fig. 4.** (a) Raised morphological markers of the Holocene paleo-sea level occurring along the carbonatic reef of Punta Gamba di Donna; LS: lower shoreline; US: upper shoreline. (b) Punta Cirucco: fossiliferous beach deposit belonging to the upper paleo-shoreline. (c) Punta Cirucco: band of fossil barnacles (*Chthamalus depressus*) belonging to the lower shoreline inside a small cave (see detail in inset). (d) Punta Gamba di Donna: fossil barnacle band belonging to the upper shoreline. (e) Cala Sant'Antonio: bioclastic marine deposit including pottery and sherds of Roman age. (f) Punta Gamba di Donna (Piscina di Venere): fossiliferous beach deposit belonging to the upper shoreline. (g) Punta del Tono: fossil barnacle band belonging to the upper shoreline.



**Table 1** <sup>14</sup>C dating results of shell fragments collected from the Holocene paleo-shorelines in the Capo Milazzo peninsula and estimated uplift rates. Age determinations by CIRCE Laboratorium, Caserta, Italy. All samples were calibrated using the program CALIB 5.0.1 (2-sigma, marine entry; Stuiver et al., 2005). Predicted sea-level points from the Lambeck et al. (2011) model; average uplift rates provide uniform uplift over the entire period of time considered.

Site	Sample name	Coordinates	Fossil organism	Measured marker elevation (m)	Measurement time (yy/mm/dd/hh)	Tide correction (m)	Atmospheric pressure correction	Corrected marker elevation (m)	<sup>14</sup> C age, y	Calibrated <sup>14</sup> C ages, 2-calibrated error, y	Predicted sea level (Lambeck et al., 2011)	Uplift rate (mm/y)
Punta Cirucco	MIL 04	38°15.807'N 15°14.628'E	Gastropod	0.85 ± 0.10	08/05/21/11	0.34	0.00 (1013 bar)	1.19 ± 0.10	4529 ± 32	4720.5 ± 102.5	-4.399	1.184
Punta Cirucco	MIL 05	38°15.807'N 15°14.628'E	Gastropod	1.33 ± 0.10	08/05/21/11	0.33	0.00 (1013 bar)	1.66 ± 0.10	3920 ± 37	3923.5 ± 124.5	-3.392	1.287
Punta Cirucco	MIL 07	38°15.810'N 15°14.603'E	Serpulid	1.65 ± 0.10	08/06/05/9	0.32	0.00 (1013 bar)	1.97 ± 0.10	4429 ± 124	4561 ± 322	-4.059	1.321
Punta Cirucco	MIL 08	38°15.817'N 15°14.617'E	Balanid	0.60 ± 0.10	08/06/05/10	0.37	0.00 (1013 bar)	0.97 ± 0.10	1867 ± 39	1413 ± 99	-0.897	1.321
Punta Gamba di Donna	MIL 06	38°16.188'N 15°13.504'E	Balanid	2.47 ± 0.10	08/11/11/8	0.37	0.00 (1013 bar)	2.84 ± 0.10	3843 ± 31	3791 ± 104	-3.067	1.558
Piscina di Venere	MIL 10	38°16.166'N 15°13.475'E	Gastropod	1.60 ± 0.10	08/11/11/9	0.30	0.00 (1013 bar)	1.90 ± 0.10	5765 ± 36	6184 ± 93	-6.868	1.417
Punta del Tono	MIL 11	38°14.723'N 15°14.267'E	Balanid	2.20 ± 0.10	08/11/11/13	0.12	0.00 (1013 bar)	2.32 ± 0.10	2056 ± 35	1622.5 ± 99.5	-1.091	2.102

shoreline" (Fig. 4a). The upper shoreline is represented by a notch, marine deposits and barnacle rims. The notch is found at ~2.1 m elevation and is carved only in the Upper Miocene limestones outcropping along the northern coast of the peninsula (Punta Gamba di Donna, Fig. 2). Well-preserved *Lithophaga* sp. holes are present on the perimeter of this notch. Locally, the notch is filled by a marine deposit formed by well-sorted coarse sands and conglomerates, including small pebbles and bioclasts of intact and fragmented shells. The average thickness of the deposit is ~0.50 m, and its top has been measured at an elevation of ~1.9 m. A rim of intertidal balanids associated to the upper shoreline has been found at a mean elevation of ~2.4 m at sheltered sites. The rim is mostly composed by the species *Chthamalus depressus* that nowadays in the Central Mediterranean Sea colonizes the meso-tidal sector and represents an important ingredient of the upper meso-littoral biocoenosis (Pères and Picard, 1964). The width of the rim typically ranges between 40 and 60 cm and reflects the combined effect of the above mean tidal range and of the locally variable wave splash zone.

The lower shoreline appears less developed/preserved than the upper one, and includes a notch and a wave-cut platform (Fig. 4a). The notch is positioned at ~0.80 m and is locally carved in the deposit of the upper shoreline. *Lithophaga* sp. holes are also observed within the notch, but they appear smaller than those associated to the upper shoreline. At the base of the notch, a wave-cut platform borders all the coast of the headland at an elevation of 0.5–0.6 m, and is particularly well developed in the northern sector. Locally, remains of a vermetid rim are found on the platform, as well as patches of a barnacle rim and a marine deposit. A living vermetid reef also occurs as a rim along the Punta Gamba di Donna coastal sector (Fig. 4a).

Below, observations on the two paleo-shorelines at three sites located along the Capo Milazzo peninsula will be described, from east to west (Fig. 2): Punta Cirucco, Punta Gamba di Donna and Punta del Tono. Discussion of each site includes the results of radiometric AMS dating. Radiocarbon ages were calibrated by the CALIB 5.0 software (Stuiver et al., 2005) that incorporates a time-dependent global ocean reservoir correction of about 400 y.

### 3.1. Punta Cirucco

Punta Cirucco is located along the northeastern coast of the peninsula (Fig. 2). In this area the rocky coast is steep, indented and highly exposed to the E-NE wind-generated waves. The two paleo-shorelines are best exposed along a small coastal headland ~100 m to the north of Punta Cirucco (Fig. 3a). The headland is orientated NNE–SSW and extends ~30 m seaward.

Along the southern corner (Fig. 3b) the upper shoreline is characterized by a fossiliferous beach deposit, by a small barnacle band and by other biological remnants. By contrast, the lower shoreline is only represented by an abrasion platform. The fossiliferous beach deposit (Fig. 4b) is heavily eroded and only a small section, about 1 m thick, with the base located at ~1.14 m elevation, is visible. The section consists of alternating sandy and gravelly layers of varying thickness containing small shell fragments and pebbles. Sediments are well sorted, although they are organized in packages of different grain size, ranging from medium to very coarse sands to granules. The finer layers show a plane-parallel lamination. Organic content is represented by abundant molluscs, benthic foraminifers and fragments of echinoids (*Paracentrotus lividus*), and subordinate bryozoan. Mollusc content is characterized by mostly encrusted and broken shells. Abundant specimens of species belonging to the biocoenosis of *Posidonia meadows* (HP) and photophilic algae (AP), such as the gastropods *Gibbula ardens*, *Jujubinus exasperatus*, *Rissoa ventricosa* and the bivalve *Venericardia antiquata* are also present. Species with wide ecological

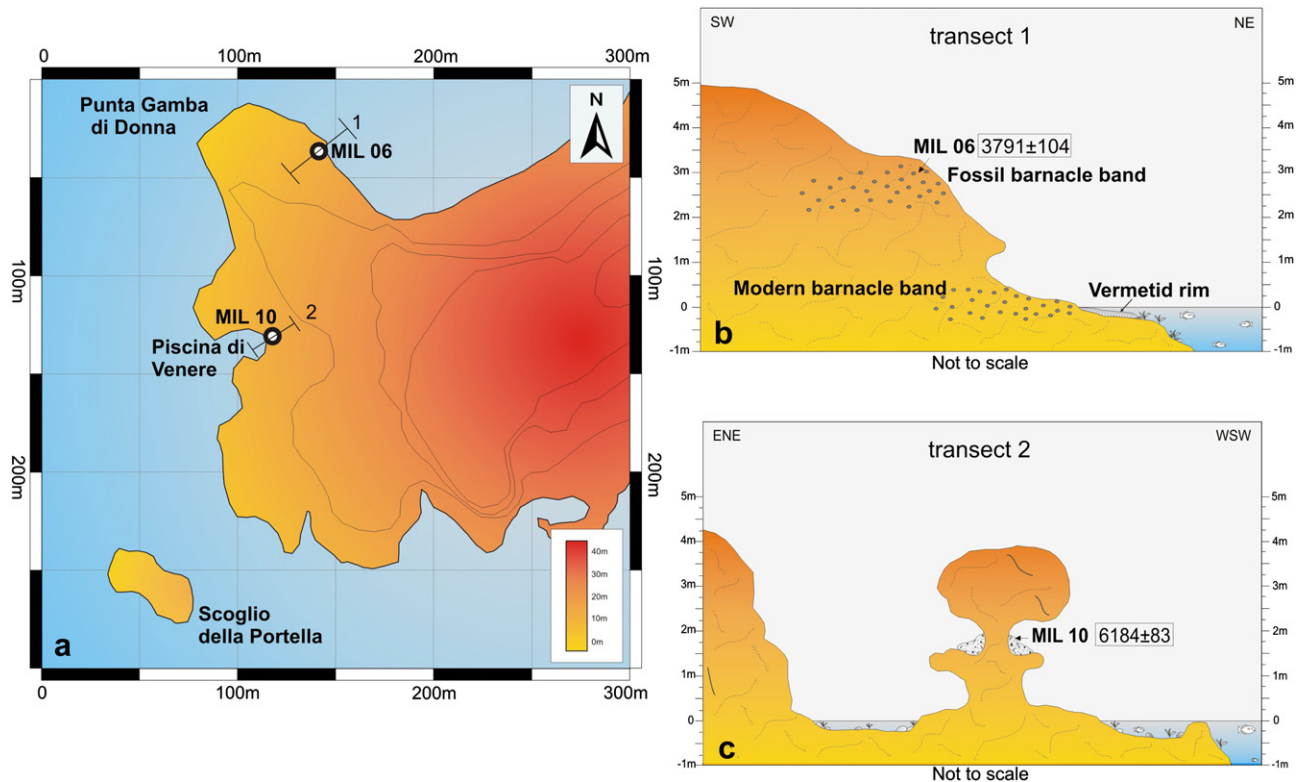


**Fig. 5.** (a) Sketch map of Punta Gamba di Donna site (see Fig. 2 for location) with location of Holocene sea-level markers (refs. Table 1). (b) and (c) Sketch profile along the southern and northern sectors of Punta Gamba di Donna, respectively, showing the morphological and biological features of the upper shoreline, their elevation above the present mean sea level and the radiometric ages of sampled organisms.

distribution such as *Bittium reticulatum* and *Cerithium vulgatum* occur in high percentages. Sedimentary features and faunal content suggest that no change in depositional conditions occurred during the time of its development, which occurred in an infralittoral beach environment. Two gastropod shells have been sampled from this deposit (MIL 04 and MIL 05; Fig. 3b and Table 1). Remains of a fossil barnacle band have been found directly above the fossiliferous beach deposits inside a cavity carved into the bedrock (Fig. 3b). The band is ~0.30 m wide, reaches an elevation of ~2.4 m and marks the maximum height of the upper shoreline at this site.

In the northern corner of the headland (Fig. 3c), the upper shoreline is totally absent, possibly because this side is more exposed to wave energy. Only serpulid encrustations were found and a sample (MIL 07; Fig. 3c and Table 1) was collected at ~1.97 m. In contrast, markers of the lower shoreline are better preserved here. The abrasion platform of the lower shoreline terminates landward in a small cave, where a barnacle band was found (Fig. 4c). The denser part of the band is ~0.2 m thick, and its top reaches an elevation of ~1.0 m marking the maximum height of the lower shoreline at Punta Cirucco. Within this band, a fossil barnacle has been sampled at 0.97 m (MIL 08; Table 1).

Radiocarbon age determinations performed on the samples collected at Punta Cirucco allow tight constraints to be placed on the age of the two paleo-shorelines (Table 1). Ages obtained for the upper shoreline range between  $4720 \pm 102$  cal BP (MIL 04) and  $3923 \pm 124$  cal BP (MIL 05). These two age determinations were performed on shells collected at the base and the top, respectively, of the fossiliferous beach deposit, and are in good agreement with their stratigraphic position. The serpulid encrustation associated to the upper shoreline must have been coeval to this deposit, because the sample MIL 07 yielded an age of  $4561 \pm 322$  cal BP. As regards

the lower shoreline, the balanid sampled from the rim yielded an age of  $1413 \pm 99$  cal BP (MIL 08).

### 3.2. Punta Gamba di Donna

Punta Gamba di Donna is a headland located at the north-western termination of the Capo Milazzo peninsula, where it extends seaward for ~300 m to the west and separates the Patti Gulf from the open sea (Fig. 2). The coast is carved into Miocene limestone, and for this reason dissolution features, such as notches, were better developed there.

Ancient sea-level markers were surveyed in this sector at several sites, namely on the eastern side of Punta Gamba di Donna, at Piscina di Venere and at Scoglio della Portella (Fig. 5a). East of Punta Gamba di Donna, both paleo-shorelines are present. The lower shoreline is represented by a wave-cut platform extending from ~1 m down to the present coastline. A ~20 cm thick barnacle band mostly represented by the species *C. depressus* was observed at a maximum elevation of 1.1 m. Similarly, the modern benthic assemblage is characterized by a band of living *C. depressus* that reaches a width of ~0.8 m, suggesting high exposure (Fig. 5b). The upper shoreline is represented by a barnacle band at elevation of 2.6–3.0 m (Figs. 5b and 4d), similar but thicker (40 cm) than that associated to the lower shoreline. A fossil balanid shell (MIL 06; Table 1) was collected from the middle portion of the upper band at 2.84 m and yielded an age of  $3791 \pm 104$  cal BP.

The Piscina di Venere (“Pool of Venus”) is a small natural pool located ~200 m south of Punta Gamba di Donna (Fig. 5a). Rust and Kershaw (2000) described two notches that are clearly distinguishable along the coastline (Fig. 4a). The lower notch is developed within an erosional relict rock located inside the pool (Fig. 5c) and



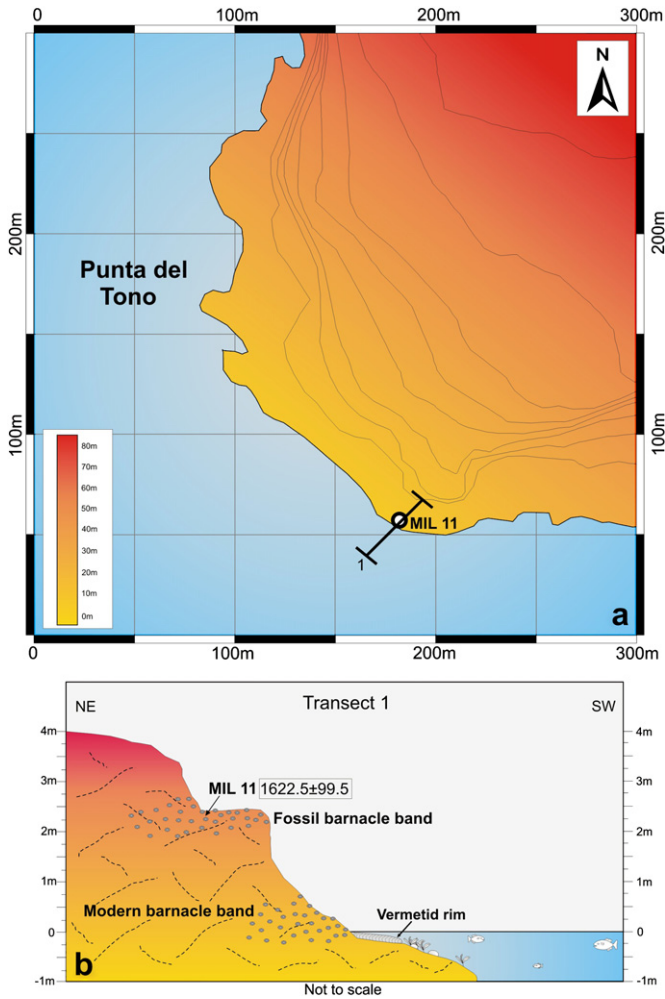


**Fig. 6.** (a) Sketch map of Punta del Tono site (see Fig. 2 for location) with location of Holocene sea-level marker (refs. Table 1). (b) Sketch profile along the southern sector of Punta del Tono, showing the morphological and biological features of the upper shoreline, their elevation above the present mean sea level and the radiometric age of sampled organisms.

along the small islet of Scoglio della Portella, 100 m offshore in front of the pool. This notch appears poorly developed/preserved and, although several lithophaga holes are present, no biological remains were found associated with the notch. The roof of the lower notch was measured at an elevation of  $\sim 0.8$  m. The upper notch is larger, better preserved and wider than the lower notch, with a roof at  $\sim 2.10$  m. In the Pool of Venus, the higher notch is filled with a marine deposit about 50 cm thick (Figs. 5c and 4e), which is formed by well-sorted coarse sands and conglomerates and includes pebbles, shells and fragments of shallow-water molluscs. A gastropod (MIL 10; Table 1), collected from the deposit at elevation of 1.9 m, yielded an age of  $6184 \pm 93$  cal BP. Several fossil barnacle bands have been found at sheltered sites (sea cavities, karst fissures), the highest of which located between 2.2 and 2.6 m.

Close to the northern corner of Cala S'Antonio, south-east of Punta Gamba di Donna (Fig. 2), the marine deposit is present at elevations from  $-0.5$  m to  $+1$  m and includes pottery and sherds of Roman age ( $\sim 2$  ka, I. Radić, personal communication) (Fig. 4f).

In summary, morphologic and radiometric results at this site document that: (i) the notch of the upper shoreline was active before  $\sim 6.2$  ka BP as shown by the gastropod MIL 10 collected from the deposit filling the upper notch; (ii) the highest horizon of the

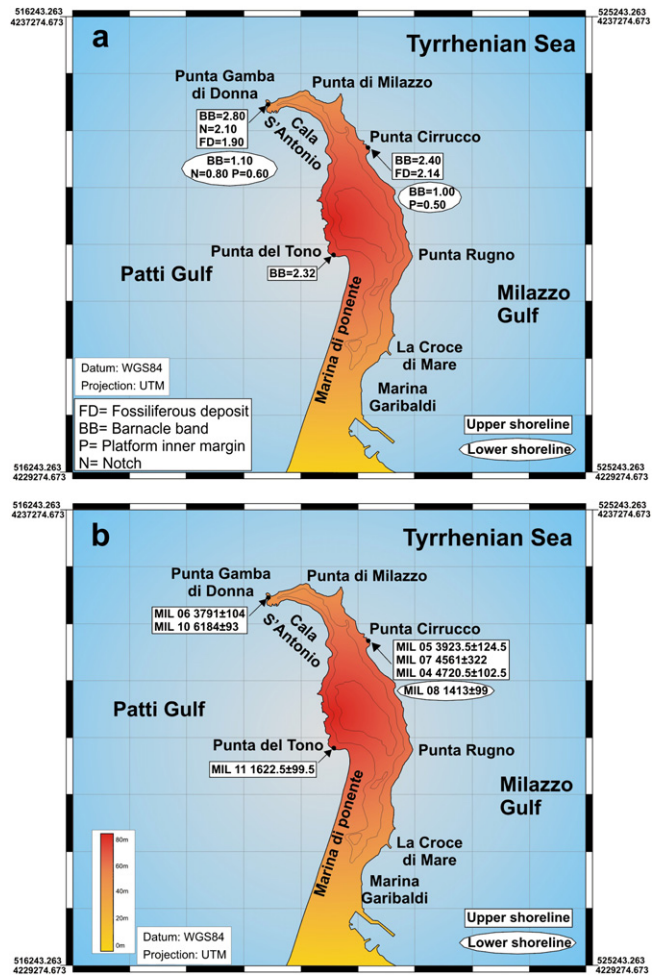


**Fig. 7.** Sketch maps of Capo Milazzo peninsula showing (a) the nominal elevation above the present mean sea level of Holocene paleo-shorelines in the distinct studied site and (b) their calibrated radiocarbon ages (in years BP).

upper shoreline corresponds to the maximum elevation of the fossil barnacle band discovered at Punta Gamba di Donna, in good agreement with the elevation of the same band at Punta Cirrucco.

### 3.3. Punta del Tono

Punta del Tono is located along the western coast of Capo Milazzo peninsula (Riviera di Ponente; Fig. 2). This stretch of coast is carved into the metamorphic bedrock and is characterized by high and indented cliffs. Due to the metamorphic nature of the bedrock, notches did not form and, similarly, abrasion platforms were not observed. In addition, blocks deposited by ancient landslides are common here, and they likely concealed or erased the morphological evidence of Holocene paleo-shorelines. Only at Punta del Tono (Fig. 6a) is the mark of an ancient shoreline represented by a prominent fossil barnacle band.

The barnacle band here (Figs. 6b and 4g) is the thickest among all those observed along the Capo Milazzo coastline, and it is quite continuous for about 400 m, encrusting the bedrock as well as the landslide blocks. The band reaches a maximum elevation of  $\sim 2.6$  m, in good agreement with that found at Punta Gamba di Donna. Similarity in elevation suggests that the barnacle band at Punta del Tono is related to the upper shoreline. As at Punta Gamba di Donna and Punta Cirrucco, the barnacles are identified as *C. depressus*. The denser part of the band, which reflects the mean tidal range, is

**Table 2**

Location and paleo-shoreline elevation at distinct sites, including tide and air pressure corrections.

Site	Coordinates	Marker	Measured marker elevation (m)	Corrected marker elevation (m)	Data uncertainty	Shoreline elevation (m)	Sea-level constraint
Upper shoreline							
Punta Cirucco	38° 15.807'N 15° 14.628'E	Balanid rim	2.07 ± 0.10	2.40 ± 0.10	±0.13	2.40 ± 0.23	Average
Punta Cirucco	38° 15.807'N 15° 14.628'E	Onlap of beach deposit	1.81 ± 0.10	2.14 ± 0.10	+0.20	2.14 +0.30 -0.10	Minimum
Punta Gamba di Donna	38° 16.188'N 15° 13.504'E	Balanid rim	2.47 ± 0.10	2.80 ± 0.10	±0.20	2.80 ± 0.30	Average
Punta Gamba di Donna	38° 16.166'N 15° 13.475'E	Onlap of beach deposit	1.60 ± 0.10	1.90 ± 0.10	+0.20	1.90 +0.30 -0.10	Minimum
Punta Gamba di Donna	38° 16.166'N 15° 13.475'E	Notch	1.80 ± 0.10	2.10 ± 0.10	±0.10	2.10 ± 0.20	Average
Punta del Tono	38° 14.723'N 15° 14.267'E	Balanid rim	2.20 ± 0.10	2.32 ± 0.10	±0.30	2.32 ± 0.40	Average
Lower shoreline							
Punta Cirucco	38° 15.817'N 15° 14.617'E	Platform inner margin	0.13 ± 0.10	0.50 ± 0.10	+0.30	0.50 +0.40 -0.10	Minimum
Punta Cirucco	38° 15.817'N 15° 14.617'E	Balanid rim	0.63 ± 0.10	1.00 ± 0.10	±0.20	1.00 ± 0.30	Average
Punta Gamba di Donna	38° 16.188'N 15° 13.504'E	Platform inner margin	0.23 ± 0.10	0.60 ± 0.10	+0.30	0.60 +0.40 -0.10	Minimum
Punta Gamba di Donna	38° 16.188'N 15° 13.504'E	Balanid rim	0.68 ± 0.10	1.10 ± 0.10	±0.20	1.10 ± 0.30	Average
Punta Gamba di Donna	38° 16.166'N 15° 13.475'E	Notch	0.5 ± 0.10	0.80 ± 0.10	±0.10	0.80 ± 0.20	Average

~0.6 m wide. Similarly, the modern shoreline benthic assemblage is characterized by a band of living *C. depressus* that reaches a width of ~1 m, indicating a high exposure area probably related to the contribution of the splash zone upon the mean tide. A fossil barnacle was collected at 2.34 m from the middle portion of the band (MIL 11; Table 1), and provided an age of 1622 ± 99 cal BP.

#### 4. Nominal age of paleo-shorelines and elevation

Cross inspection of position above the sea level and radiometric results obtained for uplifted markers allows establishment of a nominal elevation and age for the two paleo-shorelines. At each outcrop, individual markers provide different constraints on the shoreline elevation (Fig. 7a and Table 2). Whereas notches and balanid rims yield average estimations on the paleo-sea level position, platform inner margins and onlapping beach deposits furnish minimum constraints because they are formed below an unknown

**Table 3**

Nominal elevation above the present sea level and duration of the Holocene paleo-shoreline obtained by combining the individual marker elevation of dated samples (see Table 1).

Site	Nominal Elevation (m)	Shoreline onset, y BP	Shoreline end, y BP
Upper shoreline			
Punta Cirucco	2.27 +0.27 -0.17	4720.5 ± 102.5 (MIL 04)	3923.5 ± 124.5 (MIL 05)
Punta Gamba di Donna	2.27 +0.30 -0.17	6184 ± 93 (MIL 10)	3791 ± 104 (MIL 06)
Punta del Tono	2.32 ± 0.40	1622.5 ± 99.5 (MIL 11)	
Nominal age, y BP		?6184 ± 93	?1622.5 ± 99.5
Lower shoreline			
Punta Cirucco	0.75 +0.35 -0.20	1413 ± 99 (MIL 08)	
Punta Gamba di Donna	0.85 +0.30 -0.20		
Nominal age, y BP		?1622.5 ± 99.5	?1413 ± 99

depth of the water column (Table 2). In these latter cases, the uncertainty attached to the paleo-shoreline position is asymmetric, with an error of +0.30 for the platform and +0.20 for the beach deposits (Table 2). These values honour the present-day morphology of the seafloor around Milazzo and are consistent with other Holocene paleo-shoreline studies in Calabria (Ferranti et al., 2007).

Determination of the nominal elevation of the paleo-shorelines at the three studied sites derives from the integration of information provided by specific markers. At all sites, the average elevation of the upper shoreline is consistently computed at ~2.3 m (Table 3). In contrast, a slightly different nominal elevation for the lower shoreline was determined at Punta Cirucco and Punta Gamba di Donna, although within the uncertainty they could have the same elevation of ~0.9 m (Table 3).

By crossing calibrated ages obtained on all the samples collected at different sites (Fig. 7b), tight constraints can be placed on the nominal ages of the two paleo-shorelines (Table 3). At Punta Cirucco, samples MIL 04 and MIL 05, coming respectively from the base (1.19 m) and the top (1.66 m) of the beach deposit, furnished calibrated ages of 4721 ± 103 cal BP and 3924 ± 125 cal BP, respectively. The time extent of the upper shoreline can be pushed backward by the radiometric result from Punta Gamba di Donna, where the shell sample MIL 10 from the marine deposit inside the notch was dated at 6184 ± 93 cal BP. Similarly, sample MIL 06 from the same site slightly rejuvenates the shoreline at 3791 ± 322 cal BP (Fig. 7b). However, a markedly younger age for this shoreline is provided by sample MIL 11, a balanid from Punta del Tono which has a 1622 ± 99 cal BP age (Table 3). Based on these constraints, the upper shoreline was active for a minimum time span of ~4.6 ky, between ≥6.2 and ≤1.6 ka BP. However, the shoreline was slightly older than 6.2 ka, because the notch must have formed before the sediment filling it, including sample MIL 10. Based on the observation that present-day notches in the Central Mediterranean Sea take only few centuries to form (Furlani et al., 2009), the stillstand indicated by the upper shoreline had a duration of ~5 ka.

Outcrops of the lower shoreline, unfortunately, offer fewer constraints for establishing a nominal age (Table 3). The maximum age constraint for the shoreline onset is merely indicated by the

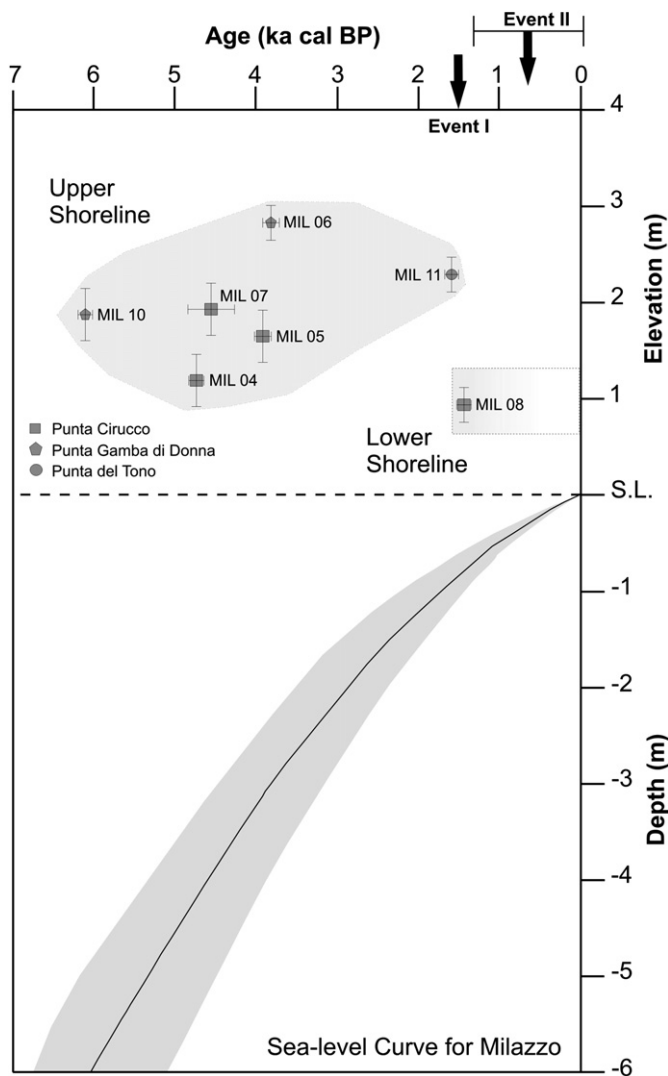


**Fig. 8.** Sea-level rise curve (thick solid line) and related  $\sigma_2$  uncertainty (grey band) for the Milazzo area according to the model of Lambeck et al. (2011). Displacement above the modern sea level, and ages of related co-seismic events I and II are also shown. The grey areas include samples from the lower and upper shorelines.

inferred cessation of the superjacent shoreline at  $\sim 1.6$  ka BP. Similarly, only sample MIL 08 dated at  $1413 \pm 99$  cal BP places a maximum age constraint for the shoreline cessation (Table 3).

### 5. Glacio-hydro-isostatic correction and uplift

In order to correctly assess the total amount of tectonic uplift experienced by the coast during the Late Holocene, accurate corrections for sea-level variations must be applied. Toward this end, the elevation-age data were compared to the local curve of Holocene sea-level rise (Lambeck et al., 2011). Using model predictions calibrated against data from 40 sites in Italy, the authors have calculated vertical motions of the crust caused by glacial and melt-water loading/unloading during the glacial cycle in addition to the global sea-level rise from the melting of the last ice sheets (the eustatic change). Of these loading corrections, the glacial signature is caused by the subsidence of the broad geoidal bulge which formed around the northern ice sheets during the last glaciation, and the melt-water signature is the subsidence induced by the weight of the melt-water on the ocean and shallow seafloor

**Table 4**  
Age and amount of co-seismic vertical displacement during Events I and II.

Event	Site	Vertical Displacement (m)
Event I (1.6-1.4 ky B.P.)	Punta Cirucco	1.52+0.31
	Punta Gamba di Donna	-0.17
Event II (post 1.4ky B.P.)	Punta Cirucco	1.42+0.30
	Punta Gamba di Donna	-0.17
		0.75+0.35
		-0.20
		0.85+0.30
		-0.20

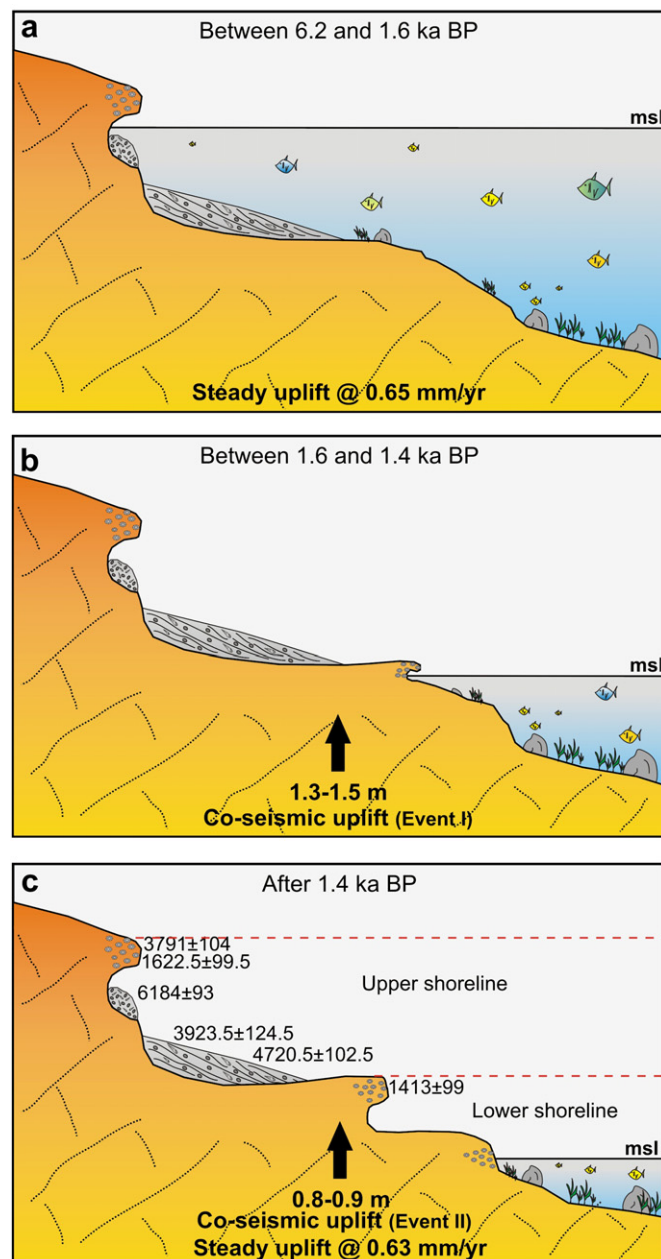


**Fig. 9.** Sketch depicting the displacement history of Capo Milazzo peninsula as integration of steady and co-seismic uplift patterns.



including the shelves. For the locations considered here, these and the eustatic contributions are additive.

The total tectonic uplift is portrayed in Fig. 8, where the dated samples collected at Capo Milazzo are grouped into two point clusters representing the upper and lower shorelines as bracketed by radiometric analysis. Inspection of Fig. 8 reveals that samples have been uplifted by an amount equivalent to their vertical distance from the sea-level curve. In Table 1 values of total uplift rate estimated for individual samples are reported. For samples from the upper shoreline, they range between  $\sim 1.2$  mm/y for the beach deposit at Punta Cirucco (MIL 04), and  $\sim 2.1$  mm/y for the balanid sampled at Punta Tono (MIL 11), with an average value of 1.5 mm/y. The balanid collected at Punta Cirucco, boarding the upper limit of the lower shoreline, provides a total uplift rate of  $\sim 1.3$  mm/y. Values calculated for both shorelines are in good agreement suggesting that the trend did not change during the Late Holocene.

## 6. Discussion and conclusions

### 6.1. Co-seismic and steady uplift of the Holocene shorelines

The coastline of Capo Milazzo offers an excellent opportunity to investigate the contribution of different processes to relative sea-level changes and cumulative tectonic displacement. The most ostensible evidence of relative sea-level change is represented by the separation of the two shorelines known from previous studies (Rust and Kershaw, 2000) and studied here in more detail. Appraisal of limiting ages suggests that distinction between the two shorelines occurred rather rapidly within a limited time window of  $\sim 200$  y between  $\sim 1.6$  and  $1.4$  ka BP. The radiometric results are in agreement with the observation that the two shorelines always show a clear spatial segregation. This separation cannot be related to a eustatic fall, because the historical sea-level curve shows uninterrupted rising (Fig. 8). On these grounds, abrupt land uplift occurred during this time window, and it was likely related to a co-seismic event that displaced the upper shoreline above sea level and set the conditions for commencement of the lower shoreline. The magnitude of the vertical displacement occurred during this event ranges from  $\sim 1.4$  to  $\sim 1.5$  m at Punta Cirucco and Punta Gamba di Donna, respectively (Event I in Table 4).

Similarly, the observation that the lower shoreline is also clearly separated from the modern shoreline points to a younger co-seismic event of uplift. Unfortunately, evidence of this younger motion cannot be provided by radiometric dating, because no age constraint exists for shoreline cessation and onset of the modern shoreline. Toward this hand, stipulation of the realistic amount of regional uplift experienced by both shorelines, in addition to the co-seismic uplift, is of use. The fact that the upper shoreline remained at a rather constant position of  $\sim 2.3$  m above the present sea level throughout its lifespan of  $\sim 4.6$ – $5$  ka, when the eustatic curve was steadily rising, suggests that a mechanism was operating to create a relative stillstand. Similar evidence was found in the Messina Strait (Fig. 1) by Ferranti et al. (2007), who suggested that steady, regional uplift must have occurred at a rate broadly coincident to that of the sea-level rise in order to maintain a fixed position of uplifted Holocene shorelines. Following Ferranti et al. (2007), the Capo Milazzo paleo-shoreline was steadily uplifted at the rate of local sea-level rise (Fig. 8).

A more accurate estimation of the steady uplift occurred at Capo Milazzo during development of the upper shoreline can be performed through stipulation of an admissible sedimentation rate for the marine deposit at Punta Cirucco. At this locale, the rate of sediment accumulation is provided by the age difference (0.80 ka) and vertical separation (0.46 m) of samples MIL 04 and MIL 05 (Table 1) which are positioned at the base and the top of deposit

(Fig. 3b). These data yield a sedimentation rate of  $\sim 0.6$  mm/y. During the same time interval ( $\sim 4.7$ – $3.9$  ka BP), the sea level was rising from  $-4.4$  to  $-3.4$  m below the present sea-level (Fig. 8), at a rate of  $\sim 1.25$  mm/y. The real rate of land uplift is estimated by subtracting the sedimentation rate from the isostatically-corrected eustatic sea-level rise,  $\sim 0.65$  mm/y.

Even though scarce remains of marine deposits are associated with the lower shoreline, a similar reasoning cannot be applied in this case. However, the width of the denser part of the associated barnacle band is comparable to that of the living rim (Fig. 3c). Based on this, the lower shoreline was steadily uplifted at a rate equal to the sea-level rise (0.63 mm/y), before being abruptly isolated above the sea by a co-seismic event. Following the discussion for the upper shoreline, the co-seismic vertical displacement of the lower shoreline can be estimated by considering the magnitude of steady uplift at Capo Milazzo and the total uplift of the younger barnacle band found at Punta Cirucco (MIL 08). The post-1.4 ka steady uplift estimated at 0.63 mm/y would have displaced the barnacle band of about 0.9 m above its physiological position. However, the sea level during the last 1.4 ka has risen about 0.89 m, and as a consequence the barnacle band found at Punta Cirucco should have remained close to the present sea-level position. Therefore, its actual location implies a displacement ranging between 0.75 and 0.85 m (Event II in Table 4).

Estimations of steady uplift for the two shorelines, using different approaches, are strikingly similar, suggesting that this inter-seismic deformation was caused by a regional process. Support toward this inference come from the elevation of the MIS 5.5 shoreline at Capo Milazzo ( $\sim 90$  m), which yields a long-term uplift at  $\sim 0.7$  mm/y (Ferranti et al., 2006). This rate should represent the cumulative effect of regional and abrupt (co-seismic) tectonic displacement at the  $\sim 100$  ka scale. If this assumption is valid, the 0.7 mm/y long-term uplift is in large part due to the regional process. The fact that in the long-term, the local, co-seismic tectonic signal is lost was previously noted in the Messina Strait by Ferranti et al. (2007), who suggested that clusters of earthquakes occurred episodically and were separated by longer quiescence intervals, when only the regional uplift operated. Accordingly, co-seismic uplift at the Capo Milazzo coastline is not constant, rather it is punctuated.

### 6.2. Late Holocene displacement history

Integration of steady and co-seismic uplift patterns indicates the history of displacement at the Capo Milazzo coastline (Fig. 9). Between 6.2 (but probably since  $\sim 6.5$  ka) and 1.6 ka, the upper shoreline was formed (Fig. 9a). The notch was the first morphological feature that started to form some centuries before the  $\sim 6.2$  ka marine deposit commenced, filling it and halting its enlargement. Sediments accumulated steadily, as indicated by radiometric dates at  $\sim 4.7$  and  $\sim 3.9$  ka. The deposit also grew in historical time, as indicated by the Roman ( $\sim 2$  ka) pottery included in it. During this time span, the land was tectonically raised at a rate (0.65 mm/y) equal to about half the eustatic rise. Only during the short time span of notch formation it was possible that land uplift was slightly faster to maintain a perfect stillstand. Starting from at least 3.8 and until 1.6 ka, a barnacle rim was formed at the top of the deposit and even above the notch, as indicated by the rim elevation at Punta Gamba di Donna (Fig. 4c). This occurrence clearly reflects the fact that the sea was rising, even if at a reduced rate (0.9 mm/y), faster than the regional uplift rate (0.65 mm/y), so that the notch was submerged and the barnacle band formed above. The fact that the band is wider than the younger and the modern ones is related to the at least  $\sim 2$  ka lifespan of the band, during which a slight relative sea-level rise must have occurred.

Between 1.6 and 1.4 ka BP, co-seismic uplift raised the upper shoreline above sea level and the lower shoreline started to form

(Fig. 9b). Although the lower shoreline includes a notch, a barnacle rim and a marine deposit, it was less developed/preserved than the upper shoreline. This occurred because the upper shoreline developed during a longer time interval, and was uplifted a larger amount above the coeval sea level (Table 4). In addition, the observation that the lower shoreline is heavily eroded could suggest that the younger co-seismic event that uplifted this shoreline (Fig. 9c) occurred close to the shoreline inception (1.4 ka BP). A relatively old age for this event could also explain why it was omitted in the historical seismicity record (see Fig. 1b).

### 6.3. Seismotectonic implications

This study documents that two paleo-earthquakes probably occurred in the Late Antiquity with coastal displacement in the Capo Milazzo area, where historical and instrumental seismicity is less intense than in nearby sectors such as the Messina Straits (Fig. 1). The analysis of historical seismicity reveals that a few earthquakes occurred in this area within the time defined for the two events. According to Guidoboni et al. (2000), based on Libanius' chronicles, a strong earthquake probably affected northern Sicily between 350 and 363 AD. Another major event probably occurred in the second half of the VII century AD, following eruptions at the Vulcano Island (Guidoboni et al., 1994). Finally, the chronicles report, even if with many uncertainties, the occurrence of a large earthquake in eastern Sicily in the 853 AD (see Boschi et al., 1995 and references therein). This uncertainty prevents definite conclusions, and further analysis in the numerous archaeological sites of northeastern Sicily would be necessary to find new information and for a more complete evaluation of this uncertain event reported in the catalogues.

Using well-established empirical relations between surface displacement and magnitude (Wells and Coppersmith, 1994), the average vertical slip per event estimated for co-seismic events I and II (~1.4 and ~0.8, respectively, see Fig. 9) at Capo Milazzo point to  $M \sim 6-7$  earthquakes, which in turn is broadly compatible with crustal structures having ~10–40 km length. What remains unsolved is the causative source for these earthquakes, which likely corresponds to an offshore fault. In this area, the transition from crustal extension in the east to shortening in northwest Sicily occurs via a belt of strike-slip and transpressive faults (Fig. 1), and is indicated by structural studies, seismicity and geodetic analysis (e.g. D'Agostino and Selvaggi, 2004; Neri et al., 2005; Pondrelli et al., 2006; Billi et al., 2006; Ferranti et al., 2008; Mattia et al., 2008). In the immediate northwest offshore of Capo Milazzo, earlier extensional structures were reactivated in a dextral transpressional regime related to N–S active compression (Mattia et al., 2009). Two active anticlines, with NW–SE striking en-echelon axes (Vulcano and Capo Milazzo folds; Fig. 1), are clearly shown by seismic profiles (Argnani et al., 2007). The elongated shape of the Capo Milazzo peninsula and the sub-horizontal attitude of the sedimentary succession outcropping on its top suggest that it may represent the southwards onshore extension of the Capo Milazzo anticline. Moreover, the geometry of this fold could be consistent with the required size of seismogenic sources for the two paleo-earthquakes detected along the coastline of the Capo Milazzo peninsula. Although further investigation is needed to document a direct link between offshore structure and coastal deformation, the analysis highlights the compelling need for a re-evaluation of seismic hazard in northeast Sicily.

### Acknowledgments

This work was supported by the Department of Civil Protection-INGV, through project S1 2007–2009 (grants to L. Ferranti), by the

VECTOR project funded by the Italian Ministry of Education, University and Research and by grants from University of Catania (responsible C. Monaco). We thank Irena Radic Rossi for age determination of archaeological sherds and the two anonymous reviewers for their comments that helped to clarify some aspects of the work.

### References

- Anderson, H., Jackson, J., 1987. Active tectonics of the Adriatic region. *Geophysical Journal Royal Astronomical Society* 91, 937–983.
- Antonoli, F., Kershaw, S., Rust, D., Verrubbi, V., 2003. Holocene sea-level change in Sicily and its implications for tectonic models: new data from the Taormina area, northeast Sicily. *Marine Geology* 196, 53–71.
- Antonoli, F., Ferranti, L., Lambeck, K., Kershaw, S., Verrubbi, V., Dai Pra, G., 2006. Late Pleistocene to Holocene record of changing uplift-rates in southern Calabria and northeastern Sicily (southern Italy, Central Mediterranean Sea). *Tectonophysics* 422, 23–40.
- Antonoli, F., Ferranti, L., Fontana, A., Amorosi, A., Bondesan, A., Braitenberg, C., Dutton, A., Fontolan, G., Furlani, S., Lambeck, K., Mastronuzzi, G., Monaco, C., Spada, G., Stocchi, P., Orrù, P., 2009. A review of the Holocene sea-level changes and tectonic movements along the Italian coastline. *Quaternary International* 206, 102–133.
- Argnani, A., Serpelloni, E., Bonazzi, C., 2007. Pattern of deformation around the central Aeolian Islands: evidence from multichannel seismic and GPS data. *Terra Nova* 19, 317–323.
- Bianca, M., Monaco, C., Tortorici, L., Cernobori, L., 1999. Quaternary normal faulting in southeastern Sicily (Italy): a seismic source for the 1693 large earthquake. *Geophysical Journal International* 139, 370–394.
- Billi, A., Barberi, G., Faccenna, C., Neri, G., Pepe, F., Sulli, A., 2006. Tectonics and seismicity of the Tindari Fault System, southern Italy: crustal deformations at the transition between ongoing contractional and extensional domains located above the edge of a subducting slab. *Tectonics* 25, 1–20.
- Boschi, E., Ferrari, G., Gasperini, P., Guidoboni, E., Smriglio, G., Valensise, G., 1995. *Catálogo dei Forti Terremoti in Italia dal 461 A.D. al 1980*. Istituto Nazionale di Geofisica, S.G.A., Roma.
- Catalano, S., De Guidi, G., 2003. Late Quaternary uplift of northeastern Sicily: relation with the active normal faulting deformation. *Journal of Geodynamics* 36, 445–467.
- D'Agostino, N., Selvaggi, G., 2004. Crustal motion along the Eurasia-Nubia plate boundary in the Calabrian Arc and Sicily and active extension in the Messina Straits from GPS measurements. *Journal of Geophysical Research* 109, B11402.
- De Guidi, G., Catalano, S., Monaco, C., Tortorici, L., 2003. Morphological evidence of Holocene coseismic deformation in the Taormina region (NE Sicily). *Journal of Geodynamics* 36, 193–211.
- Dewey, J.F., Helman, M.L., Turco, E., Hutton, D.H.W., Knott, S.D., 1989. Kinematics of the western Mediterranean. In: Coward, M.P., Dietrich, D., Park, R.G. (Eds.), *Alpine Tectonics*. Geological Society London Special Publication, vol. 45, pp. 265–283.
- Dumas, B., Gueremy, P., Lhenaff, R., Raffy, J., 1982. Le soulèvement quaternaire de la Calabre méridionale. *Revue de Géographie Physique et de Géologie Dynamique* 23, 27–40.
- Ferranti, L., Antonoli, F., Mauz, B., Amorosi, A., Dai Pra, G., Mastronuzzi, G., Monaco, C., Orrù, P., Pappalardo, M., Radtke, U., Renda, P., Romano, P., Sansò, P., Verrubbi, V., 2006. Markers of the last interglacial sea level highstand along the coast of Italy: tectonic implications. *Quaternary International* 145–146, 30–54.
- Ferranti, L., Monaco, C., Antonoli, F., Maschio, L., Kershaw, S., Verrubbi, V., 2007. The contribution of regional uplift and coseismic slip to the vertical crustal motion in the Messina Straits, Southern Italy: evidence from raised Late Holocene shorelines. *Journal of Geophysical Research* 112, B06401.
- Ferranti, L., Oldow, J.S., D'Argenio, B., Catalano, R., Lewis, D., Marsella, E., Avellone, G., Maschio, L., Pappone, G., Pepe, F., Sulli, A., 2008. Active deformation in Southern Italy, Sicily and southern Sardinia from GPS velocities of the Peri-Tyrrhenian geodetic array (PTGA). *Bollettino Società Geologica Italiana* 127, 299–316.
- Firth, C., Stewart, I., McGuire, W.M., Kershaw, S., Vita-Finzi, C., 1996. Coastal elevation changes in eastern Sicily: implications for volcano instability at Mount Etna. In: McGuire, W.M., Jones, A.P., Neuberger, J. (Eds.), *Volcano Instability on the Earth and Other Planets*. Geological Society of London Special Publication, vol. 110, pp. 153–167.
- Frepoli, A., Amato, A., 2000. Spatial variation in stresses in peninsular Italy and Sicily from background seismicity. *Tectonophysics* 317, 109–124.
- Furlani, S., Cucchi, F., Forti, F., Rossi, A., 2009. Comparison between coastal and inland Karst limestone lowering rates in the northeastern Adriatic Region (Italy and Croatia). *Geomorphology* 104, 73–81.
- Gasparini, C., Iannaccone, G., Scarpa, R., 1985. Fault-plane solutions and seismicity of the Italian Peninsula. *Tectonophysics* 117, 59–78.
- Ghisetti, F., 1979. Relazioni tra strutture e fasi trascorrenti e distensive lungo i sistemi Messina-Fiumefreddo, Tindari-Letojanni e Alia-Malvagna (Sicilia nord-orientale): uno studio microtettonico. *Geologica Romana* 18, 23–58.
- Ghisetti, F., Vezzani, L., 1982. The recent deformation mechanisms of the Calabrian Arc. *Earth Evolution Sciences* 3, 197–206.

- Ghisetti, F., 1984. Recent deformations and the seismogenic source in the Messina Straits (southern Italy). *Tectonophysics* 109, 191–208.
- Giunta, G., Luzio, D., Agosta, F., Calò, M., Di Trapani, F., Giorgianni, A., Oliveti, E., Orioli, S., Perniciaro, M., Vitale, M., Chiodi, M., Adelfio, G., 2009. An integrated approach to investigate the seismotectonics of northern Sicily and southern Tyrrhenian. *Tectonophysics* 476, 13–21.
- Goes, S., Giardini, D., Jenny, S., Hollenstein, C., Kahle, H.G., Geiger, A., 2004. A recent tectonic reorganization in the south-central Mediterranean. *Earth and Planetary Science Letters* 226, 335–345.
- Gringeri, G., Bonfiglio, L., Di Geronimo, I., Mangano, G., Antonioli, F., 2004. Uplifted Holocene littoral deposits in the Milazzo peninsula. *Quaternaria Nova* VIII, 141–154.
- Guidoboni, E., Comastri, A., Traina, G., 1994. Catalogue of Ancient Earthquakes in the Mediterranean Area up to 10th Century. ING, Roma, 504 pp.
- Guidoboni, E., Muggia, A., Valensise, G., 2000. Aims and methods in territorial archaeology: possible clues to a strong fourth century AD earthquake in the Straits of Messina (southern Italy). In: McGuire, W.G., Griffiths, D.R., Hancock, P.L., Stewart, I. (Eds.), *The Archaeology of Geological Catastrophes*. Geological Society of London Special Publication, vol. 171, pp. 45–70.
- Hearty, P.J., Bonfiglio, L., Violanti, D., Sazo, B.J., 1986. Age of late Quaternary marine deposits of Southern Italy determined by aminostratigraphy, faunal correlation and uranium-series dating. *Rivista Italiana di Paleontologia e Stratigrafia* 92, 149–164.
- Hollenstein, C., Kahle, H.G., Geiger, A., Jenny, S., Goes, S., Giardini, D., 2003. New GPS constraints on the Africa-Eurasia plate boundary zone in southern Italy. *Geophysical Research Letters* 30 (18), 1935.
- Jacques, E., Monaco, C., Tapponnier, P., Tortorici, L., Winter, T., 2001. Faulting and earthquake triggering during the 1783 Calabria seismic sequence. *Geophysical Journal International* 147, 499–516.
- Lajoie, K.R., 1986. Coastal tectonics. In: *Geophysics Studies Committee, Commission on Physical Sciences, Mathematics and Resources, Active Tectonics*. National Academy Press, Washington, pp. 95–124.
- Lambeck, K., Antonioli, F., Purcell, A., Silenzi, S., 2004. Sea level change along the Italian coast for the past 10,000 y. *Quaternary Science Reviews* 23, 1567–1598.
- Lambeck, K., Antonioli, F., Anzidei, M., Ferranti, L., Leoni, G., 2011. Sea level change along Italian coast during Holocene and a prediction for the future. *Quaternary International* 232, 250–257.
- Lanzafame, G., Bousquet, J.C., 1997. The Maltese escarpment and its extension from Mt. Etna to the aeolian islands (Sicily): importance and evolution of a lithosphere discontinuity. *Acta Vulcanologica* 9, 113–120.
- Lavecchia, G., Ferrarini, F., De Nardis, R., Visini, F., Barbano, M.S., 2007. Active thrusting as a possible seismogenic source in Sicily (Southern Italy): some insights from integrated structural–kinematic and seismological data. *Tectonophysics* 445, 145–167.
- Lentini, F., Catalano, S., Carbone, S., 2000. Carta geologica della Provincia di Messina. Scala 1:50 000. Provincia Regionale di Messina, SELCA, Firenze.
- Malinverno, A., Ryan, W.B.F., 1986. Extension in the Tyrrhenian Sea and shortening in the Apennines as a result of arc migration driven by sinking of the lithosphere. *Tectonics* 5, 227–245.
- Mattia, M., Palano, M., Bruno, V., Cannavò, F., Bonaccorso, A., Gresta, S., 2008. Tectonic features of the Lipari–Vulcano complex (Aeolian archipelago, Italy) from 10 years (1996–2006) of GPS data. *Terra Nova* 20, 370–377.
- Mattia, M., Palano, M., Bruno, V., Cannavò, F., 2009. Crustal motion along the Calabro-Peloritano Arc as imaged by twelve years of measurements on a dense GPS network. *Tectonophysics* 476, 528–537.
- Mazzuoli, R., Tortorici, L., Ventura, G., 1995. Oblique rifting in Salina, Lipari and Vulcano islands (Aeolian islands, southern Italy). *Terra Nova* 7, 444–452.
- Miyauchi, T., Dai Pra, G., Labini, S., 1994. Geochronology of Pleistocene marine terraces and regional tectonics in the Tyrrhenian coast of South Calabria, Italy. *Il Quaternario* 7, 17–34.
- Monaco, C., Tapponnier, P., Tortorici, L., Gillot, P.Y., 1997. Late Quaternary slip rates on the Acireale-Piedimonte normal faults and tectonic origin of Mt. Etna (Sicily). *Earth and Planetary Science Letters* 147, 125–139.
- Monaco, C., Tortorici, L., 2000. Active faulting in the Calabrian Arc and eastern Sicily. *Journal of Geodynamics* 29, 407–424.
- Neri, G., Barberi, G., Oliva, G., Orecchio, B., 2005. Spatial variation of seismogenic stress orientations in Sicily, South Italy. *Physics of the Earth and Planetary Interiors* 148, 175–191.
- Pères, J.M., Picard, J., 1964. *Nouveau manuel de bionomie benthique de la Mer Méditerranée*. Recueil des travaux de la Station Marine d'Endoume 31, 137.
- Pirazzoli, P.A., Mastronuzzi, G., Saliege, J.F., Sansò, P., 1997. Late Holocene emergence in Calabria, Italy. *Marine Geology* 141, 61–70.
- Pondrelli, S., Morelli, A., Ekström, G., Mazza, S., Boschi, E., Dziewonski, A.M., 2002. European-Mediterranean regional centroid moment tensors catalog: 1997–2000. *Physics of the Earth and Planetary Interiors* 130, 71–101.
- Pondrelli, S., Morelli, A., Ekström, G., 2004. European-Mediterranean regional centroid moment Tensor catalog: solutions for years 2001 and 2002. *Physics of the Earth and Planetary Interiors* 145, 127–147.
- Pondrelli, S., Salimbeni, S., Ekström, G., Morelli, A., Gasperini, P., Vannucci, G., 2006. The Italian CMT dataset from 1977 to the present. *Physics of the Earth and Planetary Interiors* 159, 286–303.
- Postpischl, D., 1985. Catalogo dei terremoti italiani dall'anno 1000 al 1980. In: *Consiglio Nazionale Ricerche, Progetto Finalizzato Geodinamica*. Graficoop, Bologna, p. 239.
- Rust, D., Kershaw, S., 2000. Holocene tectonic uplift patterns in northeastern Sicily: evidence from marine notches in coastal outcrops. *Marine Geology* 167, 105–126.
- Stewart, I.S., Cundy, A., Kershaw, S., Firth, C., 1997. Holocene coastal uplift in the Taormina area, northeastern Sicily: implications for the southern prolongation of the Calabrian seismogenic belt. *Journal of Geodynamics* 24, 37–50.
- Stuiver, M., Reimer, P.J., Reimer, R., 2005. Calib radiocarbon calibration, execute version 5.0.2 html. <http://calib.qub.ac.uk/calib>.
- Tortorici, G., Bianca, M., De Guidi, G., Monaco, C., Tortorici, L., 2003. Fault activity and marine terracing in the Capo Vaticano area (southern Calabria) during the Middle-Late Quaternary. *Quaternary International* 101–102, 269–278.
- Tortorici, L., Monaco, C., Tansi, C., Cocina, O., 1995. Recent and active tectonics in the Calabrian Arc (Southern Italy). *Tectonophysics* 243, 37–49.
- Valensise, G., Pantosti, D., 1992. A 125 kyr-long geological record of seismic source repeatability: the Messina straits (southern Italy) and the 1908 earthquake (MS 71/2). *Terra Nova* 4, 472–483.
- Ventura, G., 1994. Tectonics, structural evolution and caldera formation on vulcano island (aeolian Archipelago, Southern Tyrrhenian Sea). *Journal of Volcanology and Geothermal Research* 60, 206–224.
- Wells, D.L., Coppersmith, K.J., 1994. New empirical relationships among magnitude, rupture, length, rupture width, rupture area and surface displacement. *Bulletin Seismological Society American* 84, 974–1002.
- Westaway, R., 1993. Quaternary uplift of Southern Italy. *Journal of Geophysical Research* 98, 21741–21772.
- Wortel, M.J.R., Spakman, W., 2000. Subduction and slab detachment in the Mediterranean-Carpathian region. *Science* 290, 1910–1917.